Desalination and Water Treatment
www.deswater.com

14 (2010) 21–29
February

1944-3994/1944-3986
doi: 10.5004/dwt.2010.1007

Characteristics of ion exchange and filtration processes in the zeolite-enhanced membrane microfiltration

Jan Kinčl[a]*, Jiří Cakl[a], Richard Wakeman[b], Hana Jiránková[a], Petr Doleček[a]

[a]*Department of Chemical Engineering, University of Pardubice, nám. Čs. legií 565, 532 10 Pardubice, Czech Republic*
Tel. +420/777140406; Fax. +420 466 036 361; email: jiri.cakl@upce.cz
[b]*Department of Chemical Engineering, Loughborough University, Loughborough, Leicestershire LE11 3TU, United Kingdom*

Received 23 June 2009; accepted 6 November 2009

ABSTRACT

Ion exchange between the sodium ions from zeolite A and calcium ions from solution was studied as a part of planned water cleaning and softening process which combines zeolite ion exchange with constant flux membrane microfiltration. In the process the membrane provides a positive barrier to high concentrations of both natural solids and zeolite, while the added zeolite simultaneously assists in the removal of dissolved compounds such calcium divalent ions. Both the kinetics and the equilibrium were determined by measuring concentrations of Ca^{2+} ions in the liquid phase during the exchange process. The capacity of the zeolite studied (synthetic zeolite ZP-4A (SILKEM, Kidričevo, Slovenia)) was around 100 mg/g as Ca^{2+}. The ion exchange process was rapid and non-linear. The equilibrium was well described by UNILAN model and the kinetics by Ho-McKey's model. The specific resistance of zeolite filtration cake which was created on the membrane surface decreased significantly from 5.5×10^{10} m/kg to 1×10^{10} m/kg with the increasing amount of calcium ions loaded inside the zeolite particles. Measurements of ζ-potential and the size of zeolite particles have been carried out to examine the reason for the decrease of specific filtration cake resistance. ζ-potential of zeolite particles increased from -60 μV for fresh sodium loaded zeolite to nearly zero for fully calcium loaded particles. The decrease of the particles surface charge resulted in agglomeration into large clusters. The size of the original zeolite particles was in interval from 2 μm to 10 μm while agglomerates were larger than 100 μm. Filtration cake formed from these agglomerates was more permeable and the specific filtration cake resistance decreased.

Keywords: Ion exchange; Microfiltration; Zeolite; Hollow fiber; Water; Softening

1. Introduction

Water hardness removal is a necessity in many industrial applications, like reverse osmosis, boilers or cooling towers. Scaling of dissolved ions inside the reverse osmosis module greatly reduces the production of pure water. Hard water cannot be used for boilers and cooling towers due to formation of lime scale; the layer of precipitated solids with high thermal conduction resistance. Feed water has to be treated prior to these processes. Ions causing water hardness (Ca^{2+}, Mg^{2+}, Ba^{2+}, Sr^{2+}) can be lime precipitated, exchanged by sodium ions in zeolites or synthetic resins as well as scale inhibitors could be added [1,2]. Nanofiltration softening process is also alternative to lime or zeolite softening technologies. Nanofiltration membranes exhibit high rejection of divalent ions and are also capable of removing solids, bacteria, viruses, and color. Since

*Corresponding author

Presented at the Fourth Membrane Science and Technology Conference of Visegrad Countries (PERMEA 2009), Prague, 7-11 June, 2009.

nanofiltration operates at lower pressures than does for example reverse osmosis, the energy costs of nanofiltration softening are still very high.

The use of low-pressure membrane processes such as ultrafiltration and microfiltration have generally received greater attention lately in water treatment. Recent advances have led to the reduction in the cost of separation membranes and high energy cost cross-flow systems were replaced by hollow fiber cartridges operated in dead-end mode. This membrane configuration has also the advantage of high membrane surface area to footprint ratio. Although the process can help to meet stricter requirements for turbidity and microorganisms by size exclusion rejection, it does not remove dissolved compounds. Thus, the recent trend is to combine this low pressure membrane processes with some adsorption or ion exchange process to form a hybrid membrane system.

In this study we are focused on individual parts of the zeolite ion exchange softening process which is combined with constant flux membrane microfiltration. In this vacuum/suction driven process, hollow fiber microfiltration membranes are directly immersed in the raw water with dispersed zeolite. The membranes provide a positive barrier to biological impurities as well as high concentrations of both natural solids and zeolite, while the added zeolite simultaneously assists in the removal of dissolved compounds such calcium and magnesium divalent ions. Constant flux membrane operation may generate a substantial initial zeolite deposit, but its effect on subsequent deposition of water impurities may be beneficial in some circumstances by serving as a secondary membrane for particulate species which may otherwise infiltrate more deeply into the membrane pores. Once the cake is formed on the membrane surface, the cake layer offers an additional resistance for filtration and periodical membrane backflushing is necessary in this system in order to remove solids accumulated on the membrane.

Modeling of this process consists of flow model in the hollow fiber with the growth of the filtration cake and the ion exchange in the feed zeolite dispersion and the zeolite filtration cake. The specific resistance of the cake layer can be generally affected by particle characteristics, electrostatic interactions and hydrodynamics conditions of the separation process. Zeolite, with the characteristic of a rigid structure, may enhance the incompressibility of the cake layer and to reduce the specific cake resistance as well as this cake deposit may be more irreversible. Simultaneously the specific cake resistance may be affected by the level of saturation of zeolite particles by dissolved ions causing water hardness. Thus this article deals with the study of the dependence of specific filtration cake resistance on the amount of calcium exchanged. Calcium chloride solution was used for the hard water simulation. The description of equilibrium and kinetics of ion exchange between calcium ions from the calcium chloride sample solution and sodium ions present in zeolite particles is also needed and presented.

2. Theory

2.1. Ion exchange equilibrium

Ion exchange isotherms are the most important information for analyzing and designing an ion exchange process. The ion exchange capacity of zeolite depends on the properties of both water to be treated and zeolite used. Ion exchange equilibrium is usually determined experimentally and described by adsorption isotherms. Langmuir [3], Freundlich [3], Sips [4], Tóth [5], Radke-Prausnitz [6], Redlich-Peterson [7], UNILAN [8] and Branauer-Emmet-Teller [9] adsorption isotherms can be used for the fitting of experimental data. Preliminary experiments show that UNILAN equation in the form is the best choice for the synthetic zeolite used in this work.

$$n_e = \frac{n_{max}}{2m_U} \ln \frac{1 + k_U e^{m_U} c}{1 + k_U e^{-m_U} c} \quad (1)$$

Here n_e is the amount of calcium inside the zeolite particle in equilibrium with calcium concentration in the solution c, n_{max} is the maximal amount of calcium in fully saturated zeolite, kU and mU are UNILAN model parameters. Langmuir kinetics was also used for comparison.

$$n_e = \frac{n_{max} k_L c}{1 + k_L c} \quad (2)$$

2.2. Ion exchange kinetics

The kinetics of hardness removal from water by zeolite involves bulk solution transport, diffusion through the hydrodynamic boundary layer of fluid adjacent to the surface of the zeolite particle, internal particle diffusion, and ion exchange ''reactions'' between the ions. Each of these steps can be considered to be the rate limiting in the removal process. Thus ion exchange kinetics can be described by many different models. The first group of models contains equations derived by formal definition of reaction rate on the ion exchange surface. This way leads to the ion exchange rate which is the function of the driving force, i.e. the difference between actual and the equilibrium or the

maximum exchangeable amount. First-order kinetics [10], second-order kinetics [10], first-order Bhattacharya kinetics [11], Lagergren pseudo-first-order kinetics [12], Ho-McKay pseudo-second-order kinetics [13], Langmuir first-order kinetics [14] and Elovich kinetics [15] can be used to fit experimental data. For the evaluation of our experimental data we used Ho-McKay pseudo-second-order kinetics in the form

$$\frac{\mathrm{d}n}{\mathrm{d}t} = k_{\mathrm{HO}}(n_{\max} - n)^2 \tag{3}$$

where n is the amount of calcium inside the zeolite particle, t is time and k_{HO} is kinetic parameter.

The second group of models is based on diffusion in homogeneous particle or diffusion in surface layer of liquid as a limiting step. Diffusion control by liquid film is rare in mixed vessels, ion exchange is usually controlled by the particle diffusion [16]. Considering zeolite particle as a homogeneous sphere, Fick's law [17,18] can be applied on a particle with the radius r.

$$\frac{\partial n}{\partial t} = \mathrm{D}\left(\frac{\partial^2 n}{\partial r^2} + \frac{2}{r}\frac{\partial n}{\partial r}\right) \tag{4}$$

where t is time and D is diffusivity constant. This partial differential equation can be solved numerically or analytically in some special cases.

Analytical solution of this equation have been shown [17] for batch tests in stirred vessel and the assumption of a linear adsorption isotherm. There is also non linear driving force diffusion kinetic model presented by Georgiou [19]. Here we use the simplified solution [17] for the case in which equilibrium between adsorbed amount of calcium on zeolite and calcium amount left in solution is not linear. Separation factor, K, which should be constant in original model [17], is varied according to chosen isotherm and the factor thus depends on actual concentration (8). The model can be expressed as

$$n = n_{\max}\left[1 - \sum_{i=1}^{\infty}\frac{6\beta(\beta+1)e^{-\frac{\mathrm{D}q_i^2 t}{r^2}}}{9 + 9\beta + 9q_i^2\beta^2}\right] \tag{5}$$

$$\tan q_i = \frac{3q_i}{3 + \beta q_i^2} \tag{6}$$

$$\beta = \frac{V_{\mathrm{pp}}}{V_{\mathrm{p}}K} \tag{7}$$

$$K = \frac{n_{\mathrm{e}}c_{\mathrm{z}}V_{\mathrm{pp}}}{V_{\mathrm{p}}} \tag{8}$$

where q_i are roots of Eq. (6) for given β, V_{pp} is stirred volume per one particle of radius r and V_{p} volume of this particle and c_z is zeolite concentration.

2.3. Filtration cake formation

Microfiltration is held in constant pressure or constant rate dead-end mode. Concentration of solids is low, difference between feed and permeate flow rates is negligible. Filtration cake forms on the flat membrane or outer side of the hollow fiber membrane wall. Viscous flow through porous layer of the membrane and the filtration cake is described by Darcy's law. Form of this equation depends on coordinate system. For the flow through the flat porous filtration cake and membrane layer can be described as [20].

$$\Delta p = u\mu\left(\frac{l_{\mathrm{m}}}{k_{\mathrm{m}}} + \frac{l_{\mathrm{c}}}{k_{\mathrm{c}}}\right) \tag{9}$$

where Δp is pressure driving force needed to reach flow velocity (flux) u, μ is permeate viscosity, k_{m} is membrane permeability l_{m} is membrane thickness, k_{c} is filtration cake permeability and l_{c} is cake thickness. The cake permeability can be expressed [20] as

$$\frac{1}{k_{\mathrm{c}}} = \frac{\alpha_{\mathrm{c}}w_{\mathrm{c}}}{l_{\mathrm{c}}} \tag{10}$$

where α_{c} is specific cake resistance, and w_{c} is weight of the cake deposited per unit membrane area [20], which can be calculated from passed volume of feed dispersion or from filtration cake volume balance

$$w_{\mathrm{c}} = \frac{c_{\mathrm{z}}V}{A} = \rho_{\mathrm{s}}(1 - \varepsilon_{\mathrm{c}})l_{\mathrm{c}} \tag{11}$$

Here c_z is zeolite concentration, V is volume of the dispersion, A is membrane surface area, ρ_{s} is solid cake particles density and ε_{c} is cake porosity. Solving Eqs. (10) and (11) for k_{c}, conversion function between two cake descriptors (k_{c} and α_{c}) appears

$$\frac{1}{k_{\mathrm{c}}} = \alpha_{\mathrm{c}}\rho_{\mathrm{s}}(1 - \varepsilon_{\mathrm{c}}) \tag{12}$$

In the case of the usage for hollow fibers, Darcy's law can be written in cylindrical coordinates as

$$\Delta p = u\mu r\left(\frac{1}{k_{\mathrm{m}}}\ln\frac{r_{\mathrm{o}}}{r_{\mathrm{i}}} + \frac{1}{k_{\mathrm{c}}}\ln\frac{r_{\mathrm{c}}}{r_{\mathrm{o}}}\right) \tag{13}$$

where r_i and r_o are inner and outer membrane diameter and r_c is cake diameter. Cake diameter can be derived from mass balance of filtration cake

$$c_z V = \pi\left(r_c^2 - r_o^2\right) l_{HF}(1 - \varepsilon_c)\rho_s \quad (14)$$

Here l_{HF} is the length of hollow fiber. All parameters of the model of hollow fiber filtration cake formation are available by independent measurements on flat sheet membrane.

3. Experimental

3.1. General

The experiments were carried out using aqueous dispersions of synthetic zeolite ZP-4A (SILKEM, Kidričevo, Slovenia). It is a zeolite of type A with 4 Å pore diameter having the oxide chemical composition $Na_2O{\cdot}Al_2O_3{\cdot}2SiO_2{\cdot}4H_2O$ and particle size in range between 1 and 10 μm (4 μm average). Density of zeolite solids was determined to $\rho_s = 2{,}265\ kg/m^3$ using density bottle. Concentration of zeolite in dispersions studied was 5 g/L, 10 g/L or 15 g/L. Model wastewater solutions of appropriate hardness were prepared by dissolution of $CaCl_2$ in demineralized water. Concentration of calcium was determined by complexometric titration with EDTA.

3.2. Ion exchange measurements

Equilibrium and kinetic data batch experiments were conducted by adding defined quantity of zeolite into the Erlenmeyer flask containing defined volume of calcium solution of known initial concentration. Dispersion was mixed by magnetic stirrer at constant temperature of 25°C for 8 h while doing equilibrium experiments, samples were taken from the flask and filtered through 0.1 μm membrane filter and the solution was analyzed for calcium concentration. The procedure was repeated until no change of calcium concentration was observed. Kinetic experiments were conducted in similar way. To obtain concentration as a function of time samples were taken at timed intervals, filtered, and analyzed for calcium.

3.3. Particle behavior

Filtration process dominantly depends on particle surface potential indirectly measured by zeta potential (ζ, and the size of particles. Both the size and ζ-potential of zeolite particles under different pH and the level of exchanged amount of calcium were determined using Mastersizer S (Malvern Instruments, UK). Specific resistance of zeolite filtration cake was evaluated from the measurements in a filtration cell with flat microfiltration membrane. Low concentrations needed for particle size measurement were prepared by dilution of the concentrated dispersion in the same solution obtained by suspension filtration. Samples were measured using Mastersizer S (Malvern Instruments Ltd, UK), where particle size is determined by scattering of the laser ray.

Particle size was also measured by analyzing photographs obtained by optical microscope.

3.4. Specific filtration cake resistance

Specific resistance α_c of the zeolite filtration cake has been evaluated from the experimental measurements carried out in two types of apparatus. First, the permeation resistance of settled layer of zeolite particles was measured and secondly the resistance of filtration cake formed by filtration in standard stirred filtration cell was determined.

3.4.1. Permeation through the settled zeolite layer

Dispersion of zeolite loaded with defined amount of calcium was left to settle down on the membrane placed at the bottom of the cell (Fig. 1) to form a sediment layer. Then the layer was permeated under constant pressure by clarified mother liquid. Permeate flow, concentration of calcium and pH values were measured.

3.4.2. Filtration

Dispersion of zeolite and calcium chloride was poured into the upper vessel (Fig. 2) and stirred to reach the ion exchange equilibrium and to prevent sedimentation. Valve between the vessels was opened and filtration under constant pressure started. Filtration cake was formed on the membrane surface at the bottom of the lower vessel. Permeate flow was monitored during the experiment by collection into cylinder.

3.4.3. Ion exchange in already formed filtration cake

In order to study behavior of the zeolite filtration process more thoroughly the set of experiments was carried out where in the first step, the filtration cake layer of calcium free zeolite was formed on flat membrane surface by constant pressure filtration. Permeate was collected in cylinder and used for the second step. In the second step into the cylinder the calcium

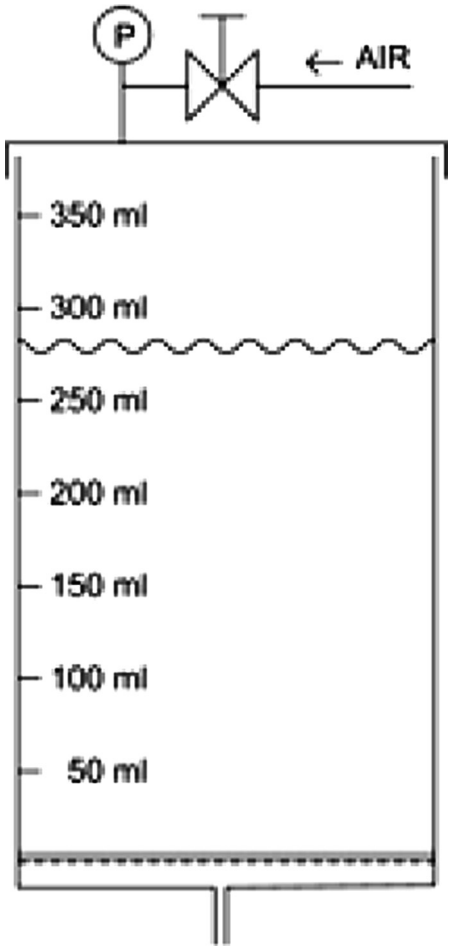

Fig. 1. Scheme of the permeation cell.

chloride was added and solution was permeated through the previously created filtration cake under the same constant pressure difference.

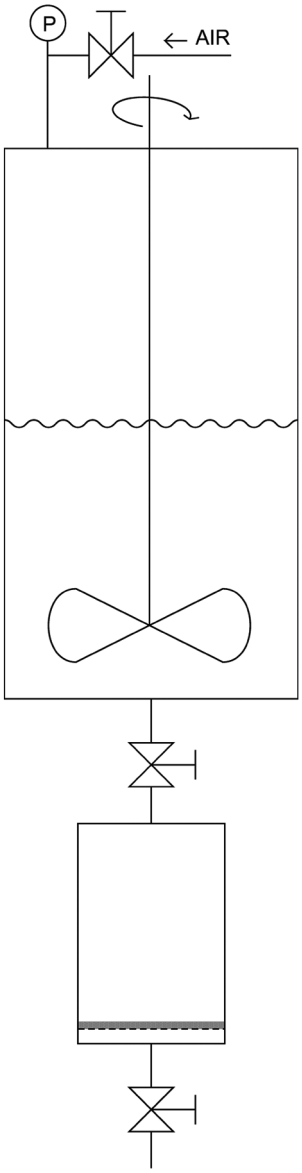

Fig. 2. Scheme of the stirred filtration cell.

4. Results and discussion

4.1. Ion exchange equilibrium

Fig. 3 shows ion exchange isotherm in model calcium solution for concentration of zeolite 5 g/l. Some of the equilibrium data were obtained also from the kinetic measurements reaching equilibrium region. First, using a Langmuir equation fit of the experimental data, the values of the isotherm parameters, n_{max} = 91.96 mg/g, k_L = 1.896 g/mg were obtained. Further the values of the UNILAN parameters n_{max} = 97.97 mg/g, k_U = 1.224 g/mg, and m_U = 5.017 were determined. It can be seen, that the three parameter UNILAN model fits the experimental data better, dominantly at lower calcium concentrations which likely occur in the demineralization process considered.

Equilibrium is strongly nonlinear. No calcium was found when solution with low initial concentration is in contact time with zeolite dispersion long enough. In the range of equilibrium concentrations higher than 200 mg/l there is only small increase in adsorbed amount of calcium. Calcium loading in the saturated zeolite is approximately 100 mg Ca^{2+} per 1 g of zeolite. It is the typical value for the type A synthetic zeolite.

4.2. Ion exchange kinetics in stirred vessel

Removal of calcium dependence on contact time with zeolite for different initial concentrations of both

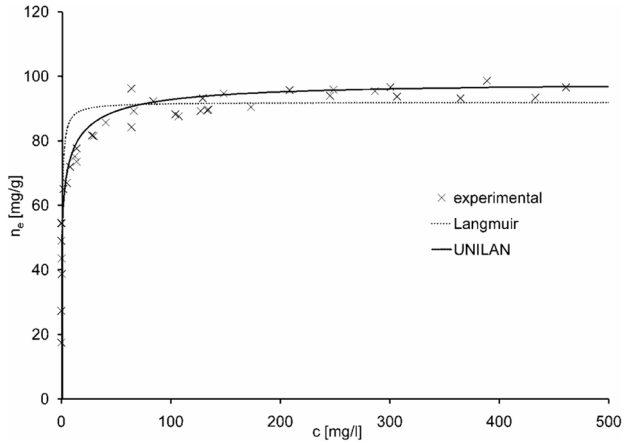

Fig. 3. Ion exchange isotherm of Ca^{2+} ions for system with Zeolite A exchanger.

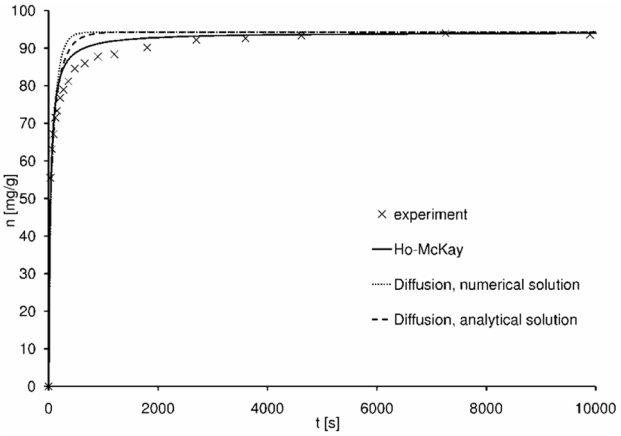

Fig. 4. Typical dependence of calcium uptake on contact time.

zeolite and calcium chloride was also studied. One example of results of kinetic measurements is shown in Fig. 4.

Ion exchange is very quick in the beginning, when relatively concentrated calcium solution and the fresh zeolite are in contact, but proceeds slowly for long time after initial rapid stage. One half of calcium is exchanged in the first 30 s but exchange still continues very slowly far after 30 min. To reach the equilibrium region at least half an hour was necessary. The effect of agitation on the kinetics was also examined for several calcium concentrations. No changes in the kinetics were observed when changing revolution from the lowest rate possible to keep dispersion homogeneous up to the highest rate possible on the magnetic stirrer. Thus it can be concluded that the surface liquid film do not add a resistance to mass transport in the systems studied and diffusion in homogeneous particle or ion exchange reaction is the mass transfer controlling mechanism. Kinetic models (Eq. (3), (4) and (5)–(8)) have been used to fit experimental data. Usually, ion exchange kinetics on zeolites is described by diffusion model, but Ho-McKay kinetics seems to fit our experimental data better. Also, diffusion model is more difficult to solve, and Ho-McKay kinetics provides solution simplicity. Parameter of McKay kinetics found for the system studied is $k_{Ho} = 3.83 \cdot 10^{-4}$ g/mg.s.

4.3. Particle properties

4.3.1. Particle ζ-potential

The results of ζ-potential measurements are depicted in Fig. 5. It can be seen that unsaturated zeolite has a highly negative ζ-potential. During the ion exchange process, ζ-potential decreases reaching minimal value at 50–60 mg of calcium per gram of zeolite. With more calcium exchanged, ζ-potential increases toward isoelectric point. This dependence may explain aggregation of zeolite particles by addition of calcium chloride as shown in Fig. 6, where particle size increases after saturation exceeds the level of 60 mg/g.

The pH value of system containing calcium chloride solution in which zeolite A is dispersed is affected dominantly by zeolite concentration and the amount of calcium already exchanged from the solution. Dispersion of unsaturated zeolite in water is alkaline having pH around 11–11.5 at zeolite concentration 5 g/l. The pH value decreases with amount of calcium exchanged. Isoelectric point is around pH 8–8.5 reached by addition of very concentrated calcium chloride (about 1 g of calcium for 5 g of zeolite in 1 L).

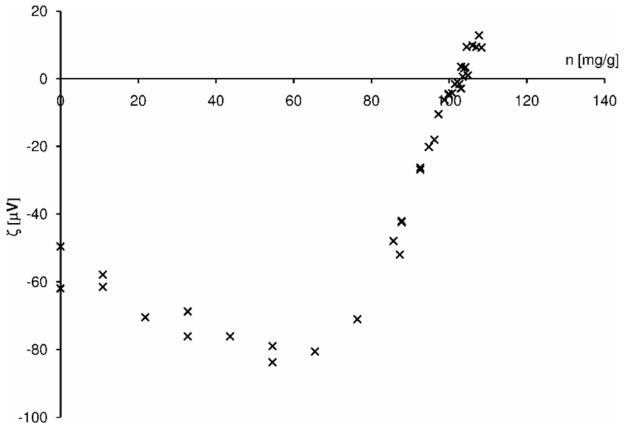

Fig. 5. ζ-potential dependence on the amount n of calcium exchanged.

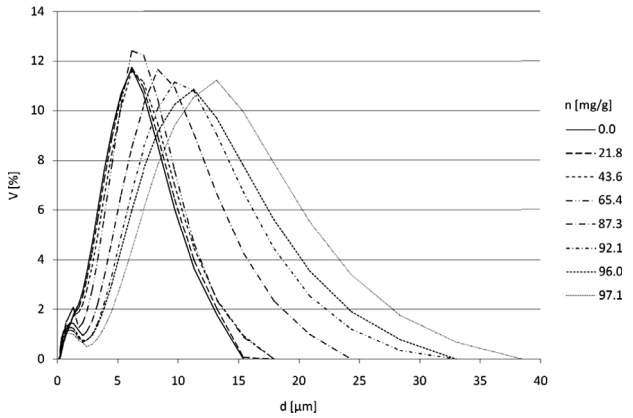

Fig. 6. Volumetric distribution of particles with size d in dependence on exchanged amount of calcium n.

4.3.2. Particle size

The size of zeolite particles changes significantly with the amount of calcium exchanged. The results of this dependence are shown in Fig. 6. Particle size is almost constant (average around 7 μm) at low amounts of calcium exchanged, but increases after calcium amount reaches 50–60 mg/g due to aggregation into large clusters. This might be caused by increasing ζ-potential up to isoelectric point on the same range of calcium saturation level. As have been said before, there is almost no calcium left in the solution if the level of exchanged calcium is below 60 mg/g (Fig. 3). Free calcium ions in the solution probably act as aggregation agent for zeolite particles decreasing their surface charge, original sodium ion seems not to have this ability.

There are mostly separated particles in dispersion of unsaturated zeolite in demineralized water (Fig. 7) and aggregates in dispersion of zeolite fully saturated by calcium (Fig. 8). Sizes of separated zeolite particles obtained by optical microscopy are close to the sizes obtained by laser scattering. The size of aggregates seem to be larger than 100 μm. Difference between sizes of aggregates obtained by laser scattering method and optical microscope can be explained by presence of the stirrer breaking the biggest aggregates in Mastersizer device.

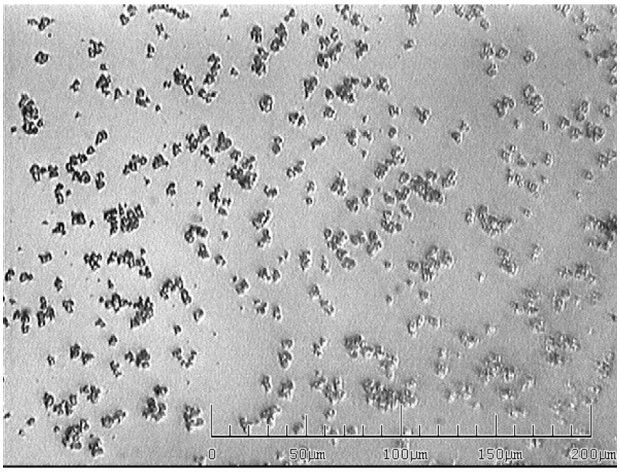

Fig. 7. Photo of unsaturated zeolite particles.

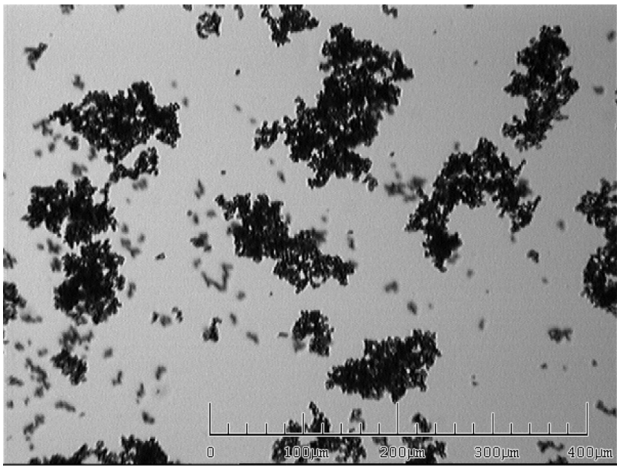

Fig. 8. Photo of saturated zeolite particles.

4.4. Specific filtration cake resistance

4.4.1. Permeation through the settled zeolite layer

The experiments on filtration cell show that the specific resistance of the sediment layer is not dependent on pressure difference used for permeation. Thus the cake layer behaves as incompressible in the range of pressures used. Dependence of α_c on the initial zeolite concentration is quite small. In contrast the relationship of α_c on exchanged amount of calcium is substantial. Specific resistance of the layer decreases from $5.5{\cdot}10^{10}$ m/kg to 10^{10} m/kg during the ion exchanges of sodium by calcium in zeolite. Logistic function in the form of fits well to the measured data. Here $\alpha_{c,0}$, k_1, k_2, n_0 are fitting parameters, $\alpha_{c,0}$ and ratio of k_1/k_2 are constants for all concentrations. Parameters obtained are summarized in Table 1.

$$\alpha_c = \alpha_{c,0}\frac{1 + k_1 e^{-\frac{n}{n_0}}}{1 + k_2 e^{-\frac{n}{n_0}}} \tag{15}$$

4.4.2. Filtration

Darcy's law based model (Eqs. (9)–(11)) was used to fit the resulting dependence of flux versus time. The membrane resistance determined from pure water

Table 1
Logistic function parameters

	$\alpha_{c,0}$ [m/kg]	k_1 [–]	k_2 [–]	n_0 [mg/g]
5 g/L	$1.198 \cdot 10^{10}$	$1.395 \cdot 10^{5}$	$3.128 \cdot 10^{4}$	6.339
10 g/L	$1.198 \cdot 10^{10}$	$0.270 \cdot 10^{5}$	$0.606 \cdot 10^{4}$	6.267
15 g/L	$1.198 \cdot 10^{10}$	$0.164 \cdot 10^{5}$	$0.367 \cdot 10^{4}$	5.776

flow measurements was used as a parameter and specific cake resistance α_c was evaluated. Filtration cake porosity was determined from the cake height at the end of an experiment using vernier caliper. Average porosity of the zeolite filtration cake was $\alpha_c = 0.532 \pm 0.055$. No dependence of the porosity on filtration pressure difference or exchanged amount of calcium in zeolite or zeolite initial concentration was observed.

There is a difference in the course of curves determined from experiments in filtration and sedimentation modes (Figs. 9 and 10). The values of the specific cake resistances are in both cases comparable in order of magnitude and decrease with increasing amount of calcium exchanged. But the shapes of the curves differ significantly. The difference may be caused by different cake layer structure. The nature of sedimentation process causes a gradient of particle sizes inside the settled layer. The largest particles forms a cake near the membrane and the smallest ones settle on the top the cake while in the filtration mode the cake is much more homogeneous.

Dependence of specific resistance of both the filtration cake and the settled layer correspond with ζ-potential data and particle size data. ζ-potential increases from minimum value to zero between 60 and 100 mg/g. Particle aggregation takes place in the same range. Larger particles form more permeable cake, thus reducing specific resistance of the layer.

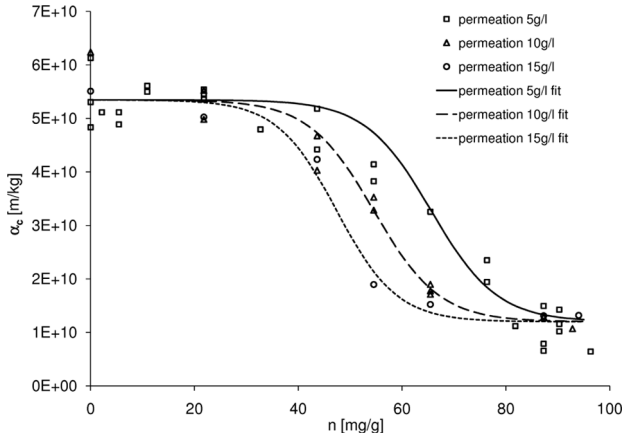

Fig. 9. Specific resistance α_c of a layer of zeolite sediment in dependence on exchanged amount of calcium n for various initial zeolite concentrations (determined from sedimentation tests).

4.4.3. Ion exchange in already formed filtration cake

No change in the filtration cake resistance was observed during experiments done by permeation of calcium solution through fresh zeolite cake layer. The results show that ion exchange in previously created filtration cake does not affect specific resistance of the filtration cake.

5. Conclusion

Ion exchange between the sodium ions from zeolite A and calcium ions from solution was studied as a part of planned water cleaning and softening process which combines zeolite ion exchange with constant flux membrane microfiltration.

The load of calcium in saturated zeolite is around 100 mg/g, which is a usual value for type A zeolite. This value gives good base for combined demineralization process considered above. Ion exchange equilibrium is highly non-linear and can be well described by UNILAN equation. Exchange process between the sodium ions from zeolite A and calcium ions from solutions is very quick at the beginning; one half of

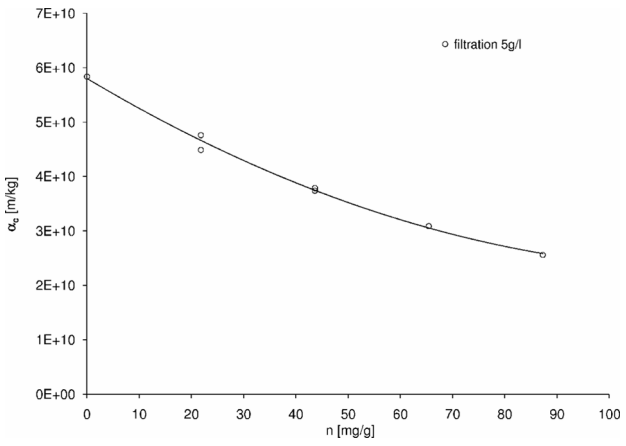

Fig. 10. The specific resistance of zeolite filtration cake α_c in dependence on exchanged amount of calcium n (calculated from filtration tests).

calcium is exchanged in first 30 s, but proceeds slowly for quite a long time. Analyses have shown that the exchange processes behavior can be described by Ho-McKay's pseudo-second order kinetic model.

The specific resistance of the cake layer created on the membrane surface by Zeolite A particles is affected dominantly by particle size and electrostatic interactions. Rigid structure of zeolite enhances the incompressibility of the cake layer and reduces the specific cake resistance. Filtration of zeolite saturated by calcium is much easier then filtration of unsaturated one. Specific cake resistance decreases with amount of exchanged calcium from 5.5×10^{10} m/kg for fresh zeolite filtration cake to 1×10^{10} m/kg for saturated zeolite filtration cake due to aggregation of fine zeolite particles into clusters which can be larger than 100 μm. Measurements of particle sizes and ζ-potential correspond with the increase of cake permeability to the large extent. Once cake is deposited no change occurs in specific cake resistance with further calcium exchange.

Symbols

c	concentration of calcium [kg.m^{-3}]
d	diameter [m]
k	permeability [m^{-2}]
k,m	various constants in models of adsorption equilibrium and kinetics
k_1,k_2,n_0	parameters of Eq. (15)
l	thickness, length [m]
n	exchanged amount of calcium [–]
p	pressure [Pa]
r	radius [m]
R	flow resistance [m^{-2}]
q_i	roots of Eq. (6) [–]
u	velocity [m.s^{-1}]
t	time [s]
V	volume [m^3]
w	deposited mass per unit area [kg.m^{-2}]
α	specific resistance [m.kg^{-1}]
β	parameter in Eq. (7) [–]
μ	viscosity [Pa.s]
ζ	ζ-potential [V]

Subscripts

c	cake
e	equilibrium
Ho	Ho-McKay's kinetics
i	inner surface
m	membrane
max	maximal
o	outer surface
p	particle
pp	per particle
U	UNILAN equilibrium
z	zeolite

References

[1] M.M. Tlili, A.S. Manzola and M. Ben Amor, Optimization of the preliminary treatment in a desalination plant by reverse osmosis, Desalination, 156 (2003) 69–78.

[2] C. Tzotzi, T. Pahiadaki, S. G. Yiantsios, A. J. Karabelas and N. Andritsos, A study of $CaCO_3$ scale formation and inhibition in RO and NF membrane processes, J. Membr. Sci., 296 (2007) 171–184.

[3] R.I. Masel, Principles of Adsorption and Reaction on Solid Surfaces, Wiley-Interscience, New York, (1996).

[4] R. Sips, On the structure of a catalyst surface, J. Chem. Phys., 16(5) (1948) 490–495.

[5] J. Tóth, State equations of the solid-gas interface layers, Acta Chim Acad Sci Hungar, 69(3) (1971) 311–328.

[6] C.J. Radke and J.M. Prausnitz, Adsorption of organic solutes from dilute aqueous solution on activated carbon, Ind. Eng. Chem. Fund., 11(4) (1972) 445–451.

[7] O. Redlich and D.L. Peterson, A useful adsorption isotherm, J. Phys. Chem., 63(6) (1959) 1024.

[8] J.M. Honig and L.H. Reyerson, Adsorption of nitrogen, oxygen, and argon on rutile at low temperatures; Applicability of the concept of surface heterogenity, J. Phys. Chem., 56(1) (1952) 140–144.

[9] D.D. Do, Adsorption Analysis: Equilibria and Kinetics, Imperial College Press, London, 1998.

[10] H. Jiránková, J. Cakl, O. Markvartová and P. Doleček, Combined membrane process at wastewater treatment, Separ. Purif. Tech., 58(2) (2007) 299–303.

[11] A.K. Bhattacharya and C. Venkobachar, Removal of cadmium(II) by low cost adsorption, J. Environ. Eng.-ASCE, 110(1) (1984) 110–122.

[12] S. Lagergren, Zur theorie der sogenannten adsorption gelöster stoffe, Kungliga Svenska Vetenskapsakademiens Handlingar, 24(4) (1898) 1–39.

[13] Y.S. Ho and G. McKey, A comparison of chemisorption kinetic models applied to pollutant removal on various sorbents, Trans. Inst. Chem. Eng., 76(B) (1998) 332–340.

[14] H. Jiránková, P. Doleček, B. Šiška and J. Cakl, Removal of organic dyes from aqueous solution by powdered acrivated carbon adsorption combined with membrane microfiltration, Scientific Papers of the University Pardubice Series A, 13 (2007) 147–156.

[15] M.J.D. Low, Kinetics of chemisorption of gases on solids, Chem. Rev., 60 (1960) 267–312.

[16] F.G. Helfferich and Y.L. Hwang, Ion exchange kinetics, in: Ion Exchangers, Walter de Gruyter, Berlin, 1991, ch. 6.2.

[17] J. Crank, The Mathematics of Diffusion, Clarendon Press, Oxford, 1956.

[18] R.M. Barrer, R.F. Bartholomew and L.V.C. Rees, Ion exchange in porous crystals, Part I. self- and exchange-diffusion of ions in chabazites, J. Phys. Chem. Solid, 24 (1963) 51–62.

[19] A. Georgiou, Asymptotically exact driving force approximation for intraparticle mass transfer rate in diffusion and adsorption processes: nonlinear isotherm systems with macropore diffusion control, Chem. Eng. Sci., 59 (2004) 3591–3600.

[20] L. Svarovsky, Solid-liquid Separation, 4th ed., Heinemann, Butterworth, 2001.